

Improving the Shunt Active Power Filter Control Methods under Distorted and Unbalanced Grid Voltages

Dinut-Lucian Popa, Petre-Marian Nicolae

University of Craiova / Electrical Engineering, Energetic, and Aeronautics Dept., Craiova, Romania,
lpopa@elth.ucv.ro, pnicolae@elth.ucv.ro

Abstract— For a proper operation of the shunt active power filters, the current reference detection method must be robust. This means it must extract correctly the fundamental frequency even if the grid has distorted and unbalanced voltages at the point of common connection. The most used reference current detection methods for shunt active power filters are analyzed and compared in this article, theoretically and through simulations in MATLAB/Simulink. One used criteria like settling time, transient performance, THD of reference and compensated grid current, overshoot and unbalance. Some practical aspects of hardware implementation and shunt active power filter design considerations are also discussed. Measured data, acquired with a dedicated data acquisition system provides the parameters required for a non-ideal real system simulation, namely a static excitation system of a power generator group. The simulated system consists of a transformer which feeds a Silicon Controlled Rectifier bridge. The Matlab/Simulink models allows for testing of the reference current detection methods implementation and improvement for dealing with problems arising with distortion and unbalance of mains voltages. Because the active power filter is a complex system, the reference current detection methods are studied with their dependencies, for example the different strategy to deal with voltage distortion and unbalance. The current controller and hardware setup are preserved. The study contributes to the existing comparisons in specialized literature by testing their weaknesses in distorted and unbalanced PCC voltages and may be useful in future hardware implementation.

I. INTRODUCTION

Proper power quality indices represent a condition for normal operation of equipment. Deviations outside some limits like the ones included in harmonic regulations or guidelines such as IEEE 519-1992 and IEC 61000 may result in thermal, reliability and economical effects with negative impact [1].

The active power filters (APFs) improve the filtering efficiency and solve some of the problems of classical passive filters (passive solutions are not effective for applications in which the nonlinear load exhibits fast transients and their performance strongly depend on the source impedance). For proper implementation of an APF, a robust method for current reference detection must be used. Some problems might arrive in calculation of reference current for the active filter, mainly due to distorted and unbalanced voltages at the point of common connection (PCC), leading to poor performance [1]-[4].

Dedicated simulation software like MATLAB/Simulink with accurate equivalent models can provide a good insight on the behavior of APF with different current control strategies.

II. POWER QUALITY MEASUREMENTS FOR THE STATIC EXCITATION SYSTEM WITHOUT COMPENSATION

The electric equivalent scheme for the simulated system is depicted by Fig. 1 [1], where the energy source is a 330 MW, 24kV three-phase synchronous generator.

The excitation system of the synchronous generator is supplied from the main terminals through a 24/0.65 kV step-down transformer by a three-phase silicon controlled rectifier (SCR) bridge.

Monitoring system's own group current measuring transformers (CMT) and voltage measuring transformers (VMT) are connected between the excitation transformer and SCR bridge. Waveforms recordings by data acquisition system are performed through these transformers [4].

The recordings were made for almost all power group quantities, but are focused mainly on the excitation transformer's secondary winding, because a strong distorting regime is encountered. Waveforms corresponding to three-phase line currents and phase voltages are depicted by Fig. 2. Original processing software packages were used for numerical processing, based on Fast Fourier Transform (FFT).

One can notice in these waveforms distorted and unbalanced currents and voltages, the perfect system for our current reference detection methods tests [1].

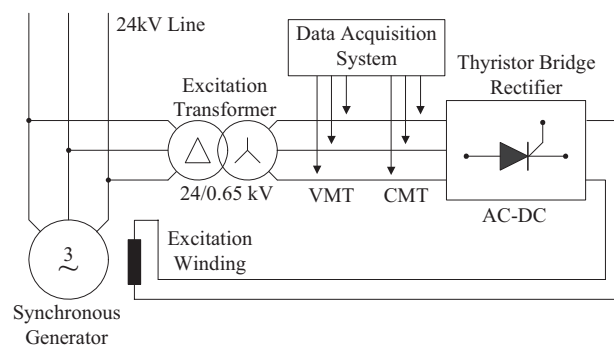


Fig. 1. Electrical equivalent scheme of the analyzed system.

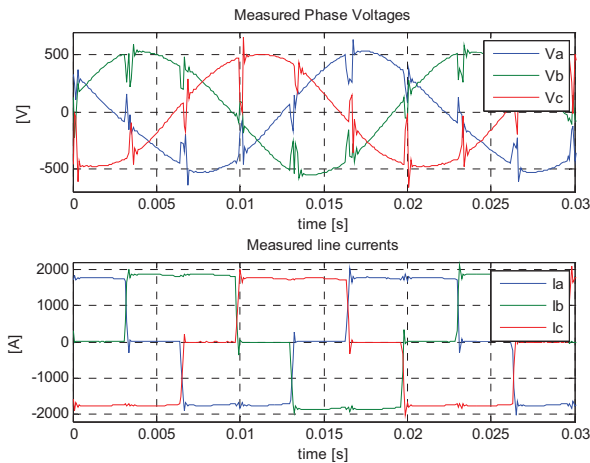


Fig. 2. Phase voltages (top) and line currents (bottom) at excitation transformer's secondary winding.

The secondary winding inductance of the transformer prevents the instantaneous transfer of current from one phase to another, resulting in two deep notches in each of the line voltages, the other four notches reflecting the action of the thyristor on the other phases. Current distortion cause is the nonlinearity of the TBR associated with the inductivity of the generator excitation winding. The main cause of voltage harmonics consists in line notches [1],[4].

The results yielded by FFT based decompositions of the voltages and currents from Fig. 2 are gathered by Table I.

The excitation system's distorting regime is significant, with a maximum total harmonic distortion factor for voltage (THDV) equal to 19.6 %, and respectively for current (THDI) equal to 29%.

The harmonic spectra of voltages and currents harmonics are depicted in Fig. 3. Typical harmonics of order $h = 6k + 1$ are present. They are characteristic to 6-pulse rectifiers. Harmonics of order 2 and 3 reveal the unbalance [1].

The maximum distorting residue of currents is 443 A and, consequently, for a full harmonic compensation, this should be the RMS current value through the APF. If power factor correction is also imposed, the current rating of APF will rise [4].

Average RMS value of currents on the three phases is 1480 A, whilst that for phase voltages is 356 V, corresponding to the rated generator operation.

TABLE I.
SIGNIFICANT PHASE VOLTAGES AND CURRENTS HARMONICS AT THE
EXCITATION TRANSFORMER'S SECONDARY WINDING

Harmonic order	Phase Voltages [% of fundamental]			Currents [% of fundamental]		
	VA	VB	VC	IA	IB	IC
2	6.17	3.15	3.71	0.88	1.68	0.78
3	3.3	2.29	4.76	0.46	0.88	0.41
5	3.99	4.21	4.82	20.72	20.12	20.17
7	4.80	4.18	4.93	13.44	13.83	13.85
11	4.25	4.36	4.53	9.22	8.67	8.72
13	4.38	3.87	4.95	7.11	7.45	7.48
17	4.18	4.25	4.30	5.91	5.34	5.43
19	4.38	3.90	4.55	4.73	5.05	5.16
23	3.99	3.99	3.96	4.29	3.75	3.82
25	4.04	3.72	4.52	3.44	3.71	3.85

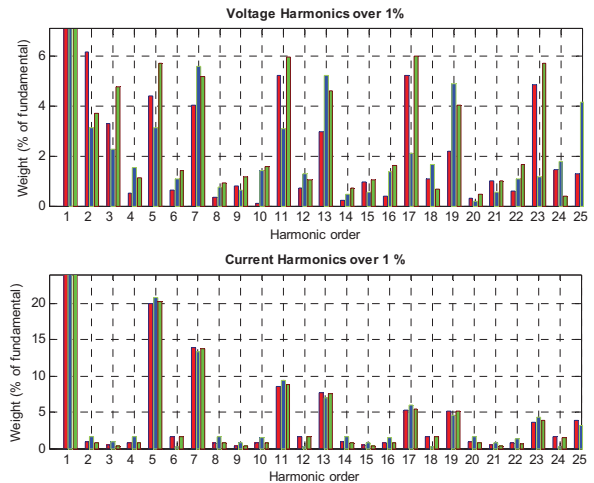


Fig. 3. Phase voltages (top) and line currents (bottom) harmonic spectra at excitation transformer's secondary winding.

The distorting residue of voltages is 66 V. The computed displacement power factor (DPF) is 0.73, corresponding to a thyristor firing angle of 45° .

III. MATLAB/SIMULINK MODEL

The MATLAB/Simulink model of the real system is built using the SimPowerSystems library. Some of the parameters are provided by measurements acquired with the data acquisition system. The system's general scheme is given in Fig. 4.

The Simulink scheme comprises the equivalent synchronous generator stator winding, the excitation transformer, the TBR with its control system and the shunt APF [4]. The active filter contains the low-power switching ripple RC filter, the high-power IGBT inverter section and the controller.

The APF controller receives as inputs the three-phase load currents, APF currents and PCC voltages, the DC-link capacitor voltage and the PWM/Compensation Enable control signals used for initialization (Fig. 10).

Two methods of implementing selective harmonic compensation (SHC) can be used. The 1st one make the Current Reference Generator (CRG) harmonic selective, whilst the 2nd one makes the Current Controller (CC) selective (in this case the whole harmonic spectrum is received at the input, but only the desired harmonic orders are regulated) [5]. The SHC technique can be used when the harmonic spectrum of the load is known (harmonics of order $h = 6k + 1$ are characteristic to 6-pulse rectifiers) so only current harmonics which exceed a certain level (recommended by standards) are removed in order to de-rate the filter inverter [1].

A. APF design considerations

The TBR input inductor is designed for a voltage drop of 3% of the mains voltage at rated current in order to limit the voltage notches and the high di/dt load values [4], [8].

The passive RC switching ripple filter is necessary to filter out the high frequency switching currents generated by the APF inverter.

When choosing the switching frequency, the RC filter switching ripple cutoff frequency must be taken into account [1], [6].

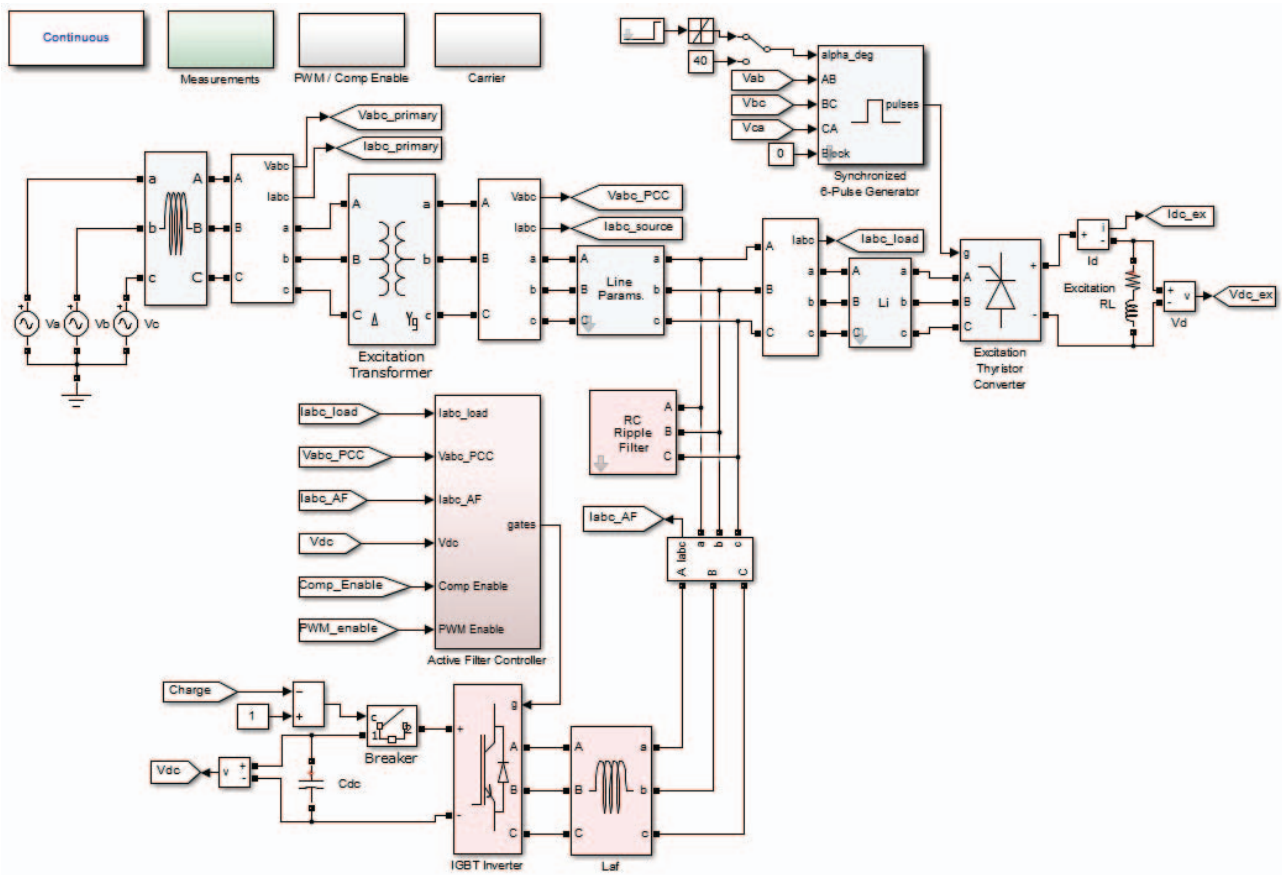


Fig. 4. The MATLAB/Simulink general scheme of the system.

The cutoff frequency of the RC switching ripple filter is computed as in (1):

$$f_{RC\ cutoff} = 1/(2\pi RC) \quad (1)$$

The cutoff frequency should be greater than ten times the fundamental frequency and lower than half the switching frequency and also less than the highest harmonic frequency to be compensated [6]. The switching frequency determines the RC filters rating hence these parameters are closely related. Considering a switching frequency of 10 kHz, a cutoff frequency of 5 kHz was selected.

The current controller is implemented by a triangular fixed carrier PWM technique. This is a constant switching frequency technique so the switching-ripple currents are defined around multiple integers of the switching frequency. Compared to variable switching techniques, the switching losses are lower and the switching ripple filter operation and cost are more efficient. The bandwidth is greatly increased by using P-SSI current controllers (Proportional-Sinusoidal Signal Integrator) with multiple SSIs in synchronous reference frame [7]. Simple PI current controllers have a lower bandwidth, being better suited for tracking sinusoidal currents [8].

Because the APF needs to inject a current with a RMS value of more than 400 A and high slopes corresponding to high di/dt load current, the APF coupling inductance is chosen as a compromise between voltage ripple and current spikes. The larger the inductance the higher are the current spikes and lower the voltage ripple.

B. APF initialization

The APF needs to be initialized in order to start correctly:

1) *The DC-link capacitor is pre-charged to peak line voltage (which is 915 V) using an 8 Ω charging resistor which is short-circuited by a breaker after 20 ms. This way the high charging inrush currents are avoided (Fig. 5).*

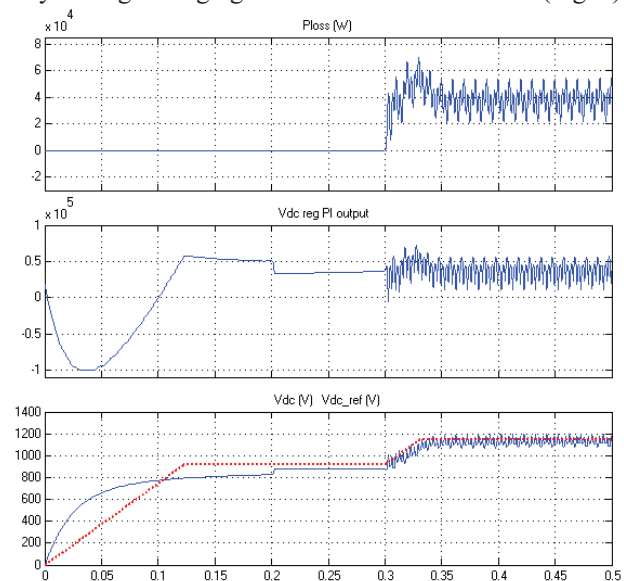


Fig. 5. DC-link voltage regulator operation: active power loss (top), PI regulator output (middle), DC-link capacitor measured voltage and reference (bottom).

2) The compensation is enabled after the capacitor is charged (Fig. 5).

3) The DC-link voltage is increased. 915 V is not enough as to control the currents that must be injected at the PCC to avoid spikes in the compensated current (Fig. 5). As compensation is enabled, the capacitor is charged to 1150 V by a gradual rising voltage reference (multiplying 1150 to a linear coefficient $k(t)$). This way a high-speed transient response can be achieved choosing more aggressive the voltage regulator proportional and integral terms. When the thyristor firing angle changes fast from low to high the capacitor voltage tends to rise over 1150 V so the voltage regulator must be tuned as a compromise between stability and voltage rise [1].

C. Future work

1) An S-function is a computer language description of a Simulink block written in MATLAB®, C, C++, or Fortran. The controller for the current simulations consists of handwritten MATLAB Level-2 S-Functions blocks excepting the digital filters and integrators. A handwritten C MEX S-function provides the most programming flexibility because the programmer has the freedom of implementing his own libraries, and lower the computational burden for the DSP. Otherwise, for complicated systems, Level-2 MATLAB S-functions and the Simulink digital filters and integrators blocks code will work slower than C MEX S-functions because they call out to the MATLAB interpreter [9]. In order to fully validate the Simulink model, the APF controller should be implemented in a DSP using a dSPACE based solution and tested in a real-time setup.

2) Considering the high power rating of the APF inverter for the current application, a structure that consists of multiple parallel inverters sharing the DC-link will be adopted because it has several advantages [10]. The most important one is that the harmonic current to be injected can be divided between the inverters, lowering the power rating proportional with the number of inverters. Another advantage is the reduction of the current ripple if the inverters have the same switching frequency, and their carrier signals are phase shifted by 180°. This minimizes the high frequency losses in the power line, the electromagnetic interference (EMI) and the size of the switching ripple filter.

IV. APF REFERENCE CURRENT DETECTION METHODS COMPARISON

In the author's opinion the APF is a complex system and the reference current detection methods need to be studied with their dependencies (for example the different system to deal with voltage distortion and unbalance or DC-link voltage regulator implementation). The current controller and hardware setup are preserved. The selected methods are analyzed and compared with respect to their performance under distorted and unbalanced PCC voltages. These may be used to decide the future hardware setup implementation. The study contributes to the existing comparisons in specialized literature by testing their weaknesses in distorted and unbalanced PCC voltages.

The studied harmonic detection methods are implemented in the time-domain and frequency-domain respectively [1].

A. Time-domain methods

The time-domain methods offer increased speed and fewer calculations compared to the frequency-domain methods because they don't use memory buffers, only a few low-pass or band-pass digital filters [11].

The instantaneous reactive power theory (IRP) determines the harmonic content by extracting the instantaneous oscillating powers (Fig. 10 a, e). First, the three-phase voltages and currents coordinates are transformed to $\alpha\beta$ using the Clarke transform [2], [12]:

$$\begin{bmatrix} u_0 \\ u_\alpha \\ u_\beta \end{bmatrix} = \sqrt{\frac{2}{3}} \begin{bmatrix} \frac{1}{\sqrt{2}} & \frac{1}{\sqrt{2}} & \frac{1}{\sqrt{2}} \\ 1 & -\frac{1}{2} & -\frac{1}{2} \\ 0 & \frac{\sqrt{3}}{2} & -\frac{\sqrt{3}}{2} \end{bmatrix} \begin{bmatrix} u_a \\ u_b \\ u_c \end{bmatrix} \quad (2)$$

Then, the instantaneous powers are computed using the $\alpha\beta$ coordinates of phase voltages and currents [2]:

$$\begin{bmatrix} p(t) \\ q(t) \end{bmatrix} = \begin{bmatrix} u_\alpha(t) & u_\beta(t) \\ u_\beta(t) & -u_\alpha(t) \end{bmatrix} \cdot \begin{bmatrix} i_\alpha(t) \\ i_\beta(t) \end{bmatrix} \quad (3)$$

Each of the two instantaneous powers contains a constant term related to the fundamental content and an oscillating term related to harmonics content [2]:

$$\begin{aligned} p(t) &= \bar{p} + \tilde{p}(t) \\ q(t) &= \bar{q} + \tilde{q}(t) \end{aligned} \quad (4)$$

In order to obtain the oscillating instantaneous power components \tilde{p} and \tilde{q} , two Butterworth 5th-order digital low-pass filters with 100 Hz cutoff frequency are used and then the oscillating powers are subtracted from the total powers (p and q) [12]. This method is insensible to the phase shift introduced by the high pass filters.

With the oscillating powers extracted, the APF compensation currents are computed with (5) [12]:

$$\begin{bmatrix} i_{c\alpha}(t) \\ i_{c\beta}(t) \end{bmatrix} = \frac{1}{v_\alpha^2(t) + v_\beta^2(t)} \begin{bmatrix} v_\alpha(t) & v_\beta(t) \\ v_\beta(t) & -v_\alpha(t) \end{bmatrix} \cdot \begin{bmatrix} -\tilde{p}(t) + \bar{p}_{loss}(t) \\ -\tilde{q}(t) - k \cdot \bar{q}(t) \end{bmatrix} \quad (5)$$

If power factor's correction is desired the operation involves the division of the constant instantaneous reactive power \bar{q} by multiplying with a factor k in order to achieve the target power factor.

A small amount of real power \bar{p}_{loss} must be continuously drawn from the supply in order to compensate for switching and ohmic losses in the PWM IGBT converter. Otherwise, this energy would be supplied by the DC-link capacitor, which would discharge.

The 100 Hz cutoff frequency of Butterworth filters is chosen such as to prevent interferences with power oscillations due to the fast firing angle variation. Also the lowest orders harmonics to compensate (3rd due to unbalance and 5th) had to be considered [1],[4], [12].

The definition of IRP theory shows that for distorted and unbalanced voltages it is impossible to obtain sinusoidal source currents and respectively draw a constant instantaneous active power [2],[12]. Figure 6 depicts an example of some distorted reference currents obtained when the phase voltages are used directly in (3), without

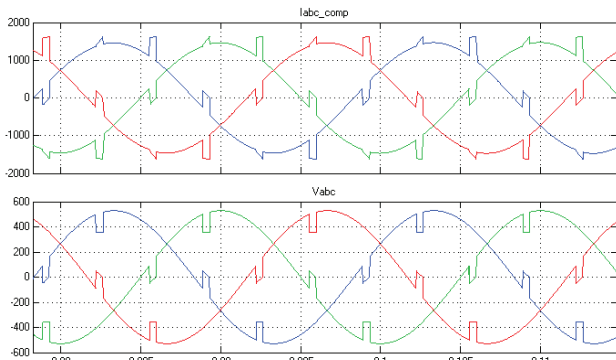


Fig. 6. Example of distorted reference currents obtained (top), when the phase voltages (bottom) are used directly without filtering.

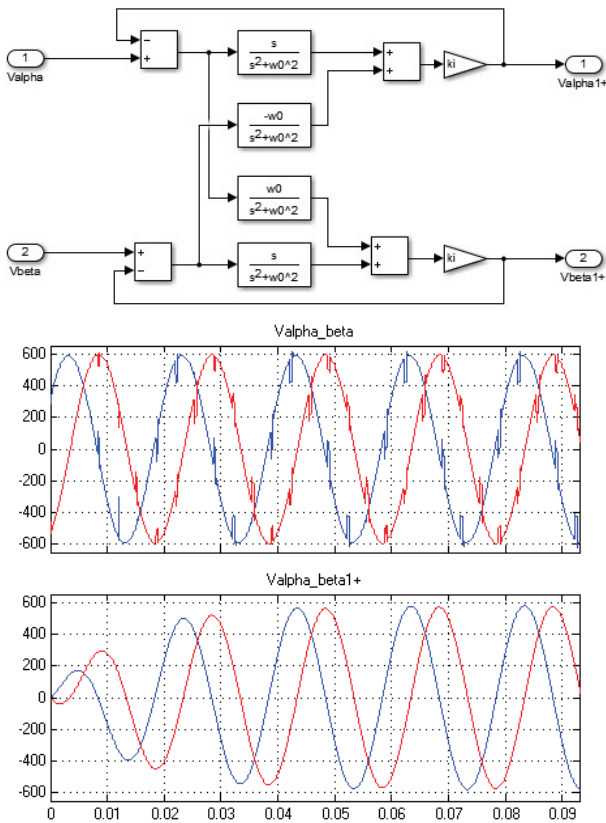


Fig. 7. The Simulink scheme of the fundamental positive sequence detector and its operation under distorted and unbalanced PCC voltages.

filtering [4]. The input voltages are distorted but balanced. If in addition they were unbalanced too, the results are expected to be worst.

The problem caused by the voltage distortion and unbalance can be solved using a fundamental positive sequence detector. This paper proposes the one in [13], which uses four SSI-s (detailed in the dedicated section).

The Simulink scheme of the detector is depicted in Fig. 7. The four transfer functions are equivalent with four SSI-s. The k_i factor is chosen low as to obtain a good accuracy and also because voltages have very slow variations.

For system where the α -axis signal always lags the β -axis signal by 90 degrees (negative sequence system) the signs for the cross-coupling terms must be exchanged. This scheme does not use trigonometric functions (filter coefficients are computed in advance) and in consequence

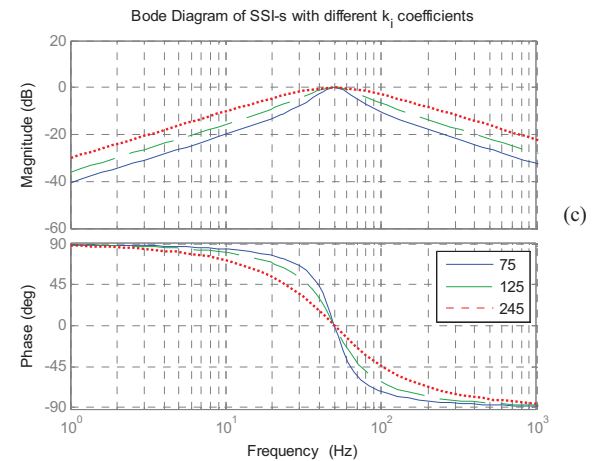
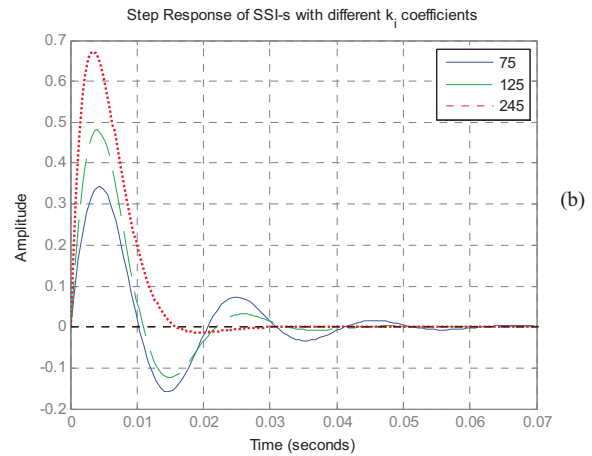
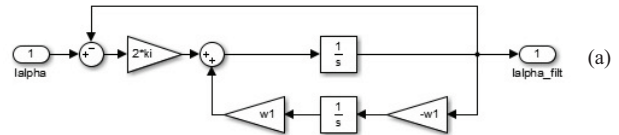


Fig. 8. Simulink model of the i_α P-SSI regulator (a), step response (b) and Bode plot (c) for different values of k_i coefficient.

it allows reducing computational resources [13].

SHC can be used by implementing an algorithm like in [14], where the voltages in (5) are synthesized harmonic voltages with angular frequency $k\omega_1$, where k is the harmonic order. The amplitude and phase of these harmonic voltages has no influence on the results. The phase of the PCC fundamental positive sequence voltage vector must be detected using a phase-locked loop (PLL) algorithm in order to compute the harmonic voltages. This SHC method uses two digital filters per harmonic and trigonometric functions, increasing the computational burden for the DSP.

The rotating (synchronous) d - q reference frame method aligned with the PCC voltage vector is similar to IRP theory, but the harmonic content is extracted from the i_d and i_q oscillating components computed with (6) (the fundamental active and reactive components of the load current and the active component to keep the dc-link capacitor charged are dc quantities) [7], [8] (Fig. 10 b, d). The same Butterworth filters with 100 Hz cutoff frequency are used.

$$\begin{bmatrix} i_q \\ i_d \end{bmatrix} = \begin{bmatrix} \cos(\theta) & -\sin(\theta) \\ \sin(\theta) & \cos(\theta) \end{bmatrix} \begin{bmatrix} i_\beta \\ i_\alpha \end{bmatrix} \quad (6)$$

This method receives as inputs the load measured currents in the stationary $\alpha\beta$ reference frame, the output of the DC-link regulator i_{d_loss} as well as the position of the PCC voltage vector θ computed by means of a voltage filter scheme consisting of an SSI and a phase-locked loop (PLL) algorithm, as in [7]. This provides a smooth and accurate position of the PCC voltage vector for the APF control scheme even under distorted and unbalanced PCC voltages (Fig. 9). The PLL is locked in less than 15 ms.

If power factor compensation is desired, the fundamental reactive reference component i_q (constant term) must be divided.

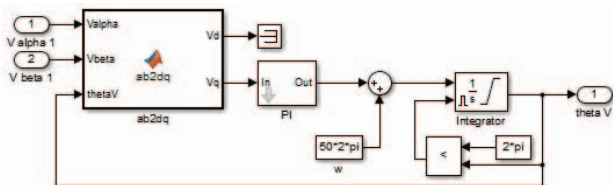
SHC is achievable by rotating the $d-q$ frame with the angular speed of the selected harmonic frequency. Thus, in the harmonic's $d-q$ frame the respective harmonic is a dc signal and all other frequencies, including the fundamental, are ac components [11].

The reference current detection method which uses stationary frame generalized integrators is based on the sinusoidal signal integrator (SSI), which tracks the load current's sinusoidal reference (with zero steady-state error) and is tuned on the fundamental frequency (Fig. 10 c, f).

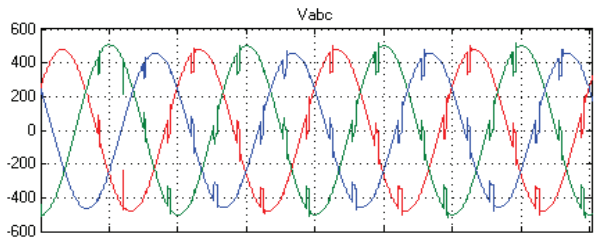
This method doesn't use the PCC voltages, but in the general control scheme those are needed by the DC-link voltage regulator. For this, a small active current in phase with the PCC voltages must be drawn, according to (7).

$$\begin{bmatrix} i_{\alpha_loss} \\ i_{\beta_loss} \end{bmatrix} = \frac{1}{v_{\alpha}^2 + v_{\beta}^2} \begin{bmatrix} v_{\alpha} & -v_{\beta} \\ v_{\beta} & v_{\alpha} \end{bmatrix} \begin{bmatrix} p \\ 0 \end{bmatrix} \quad (7)$$

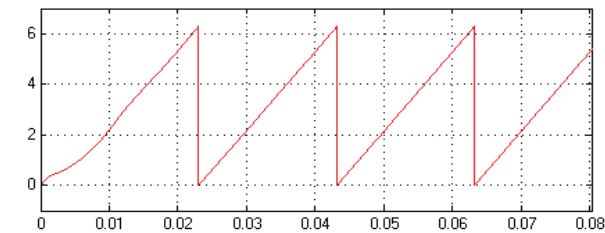
where p is the active power loss and the output of the PI voltage regulator. The SSI is able to operate with both positive sequence and negative sequence signals.



(a)



(b)



(b)

Fig. 9. The scheme of the PLL (a) and his operation under distorted and unbalanced PCC voltages (b).

In the continuous-time domain, the transfer function of a P-SSI is given by [7], [8]:

$$H_{P-SSI}(s) = k_p + \frac{2 \cdot k_i \cdot s}{s^2 + \omega^2} \quad (8)$$

where k_p is the proportional gain, k_i is the integral gain and ω is the resonant angular frequency (set for the 50 Hz fundamental frequency). Two SSI-s are used, one for i_{α} and the other for i_{β} . The filter transfer function is equivalent to the block diagram in Fig. 8. The corresponding state-space model for code implementation is described in [7].

From the step response and Bode plot of the SSI for different values of k_i (Fig. 8) one can observe that when k_i becomes smaller, the settling time gets bigger but the filter becomes more selective, so k_i must be chosen as a compromise between THD and fast response to thyristor firing angle change [1].

An improved version of the scheme in Fig. 8 would be like that from Fig. 7 which uses four SSI-s. This last one is more insensitive to unbalance and distortion as it can be seen from the simulation results, but it doubles the processing time of the DSP.

If SHC is desired, we need two SSI-s for every selected harmonic (one SSI for i_{α} and the other for i_{β}).

B. Frequency-domain methods

The frequency-domain methods are mainly Fourier based and uses memory buffers to store a number of samples N contained in a fundamental period [15]. The discrete Fourier transform (DFT) is a transformation for discrete signals which converts the time domain signal to the frequency domain spectrum, giving the amplitude I_M and phase φ_l of the selected harmonic [11], in this case the fundamental:

$$\begin{aligned} \bar{I} &= \sum_{n=0}^{N-1} x(n) \cdot \cos\left(\frac{2\pi \cdot n}{N}\right) - j \cdot \sum_{n=0}^{N-1} x(n) \cdot \sin\left(\frac{2\pi \cdot n}{N}\right); \\ \bar{I} &= \text{real}(\bar{I}) + j \cdot \text{imag}(\bar{I}); \\ I_M &= \sqrt{\text{real}^2(\bar{I}) + \text{imag}^2(\bar{I})}; \\ \varphi_l &= \arctan\left(\frac{\text{imag}(\bar{I})}{\text{real}(\bar{I})}\right) \end{aligned} \quad (9)$$

In (9), \bar{I} is the complex Fourier vector of the fundamental current and n is the sample number. For a sampling frequency of 10 kHz, the number of samples N is 200.

The output reference current based on the discrete Fourier transform takes the advantage of being a pure sinusoid. Its THD value is very low, being limited only by the number of samples used for computations.

In this paper the recursive discrete Fourier transform (RDFT) is implemented, which uses the same principle as the DFT but calculated on a sliding window which shifts with every sample time (Fig. 10 c, g).

In the sliding process, the new sample $x(n)$ is saved on the first position, and the last sample $x(n-(N-1))$ is cleared. Then, all samples are multiplied by $e^{-jn2\pi/N}$ corresponding to the first signal component (for 50 Hz) [15]. The DFT analysis can be performed with every new achieved sample but for fast varying loads the results are more likely to be imprecise due to the sliding window lag. Other drawbacks are large memory requirements to store the

achieved samples and large computation power required for the DSP [11]. Two windows are required, one for α component and the other for β but if reactive power compensation is desired also, other two sliding FFT windows for computing the voltage phases are necessary. SHC needs two sliding windows per harmonic, which means two memory buffers, significantly increasing the computational burden for the DSP. However, the needed memory buffer size decreases with the increase of the frequency (harmonic order) because the corresponding period is smaller.

The Simulink schemes of the controllers for time domain and frequency domain reference current detection methods are depicted in Fig. 10.

For the Simulink comparison one used criteria like settling time, transient performance on thyristor firing angle change (which is directly proportional with the settling time), THD of reference and compensated grid current, overshoot, unbalance and DSP computational burden. The step response is depicted in Fig. 11 and the comparison results are centralized in Table II.

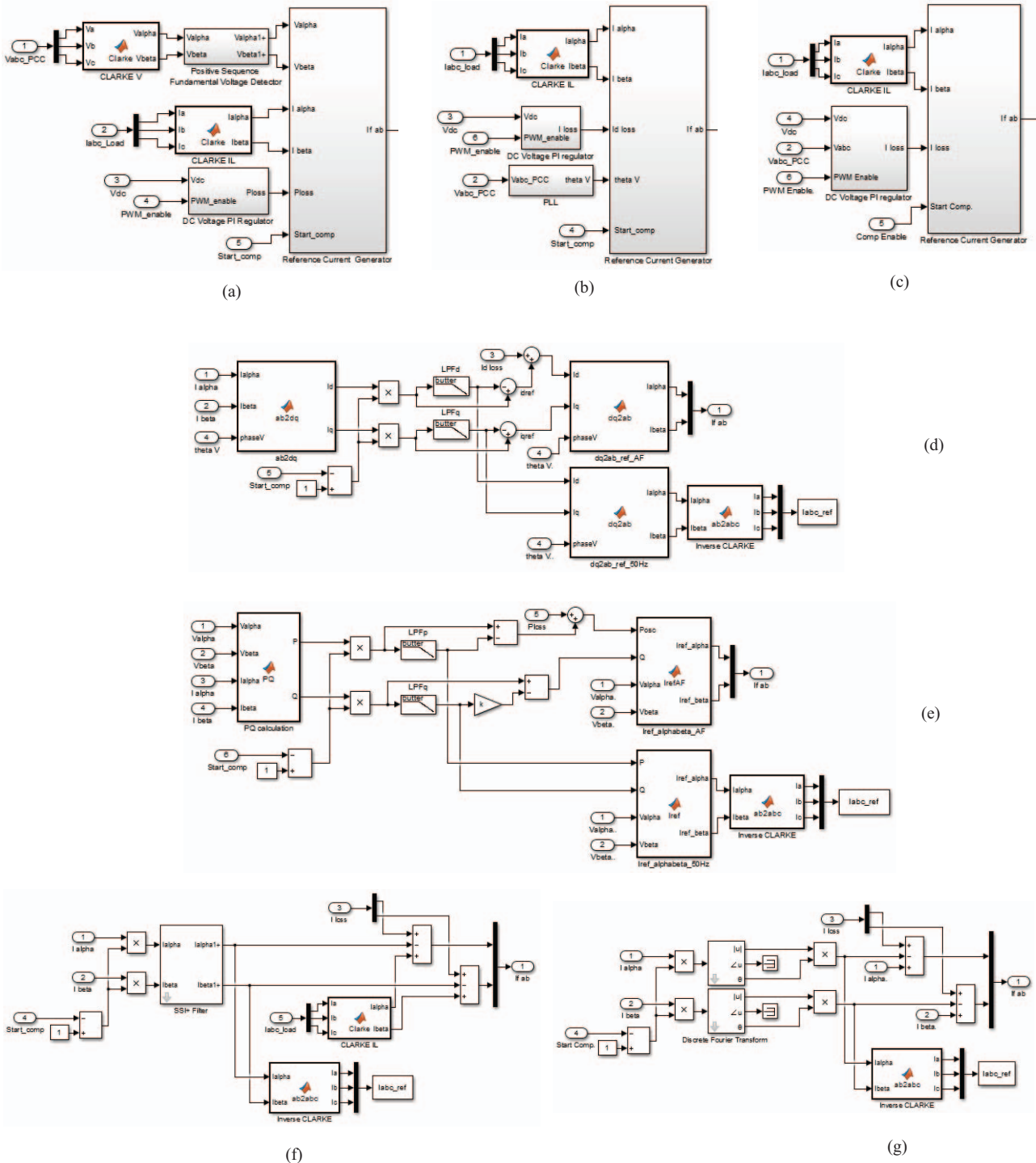


Fig. 10. The Simulink general schemes of the APF reference current detection: (a) IRP theory; (b) $d-q$ reference frame; (c) SSI, SSI+ and RDFT, and internal schemes: (d) $d-q$ reference frame; (e) IRP theory; (f) SSI and SSI+; (g) RDFT.

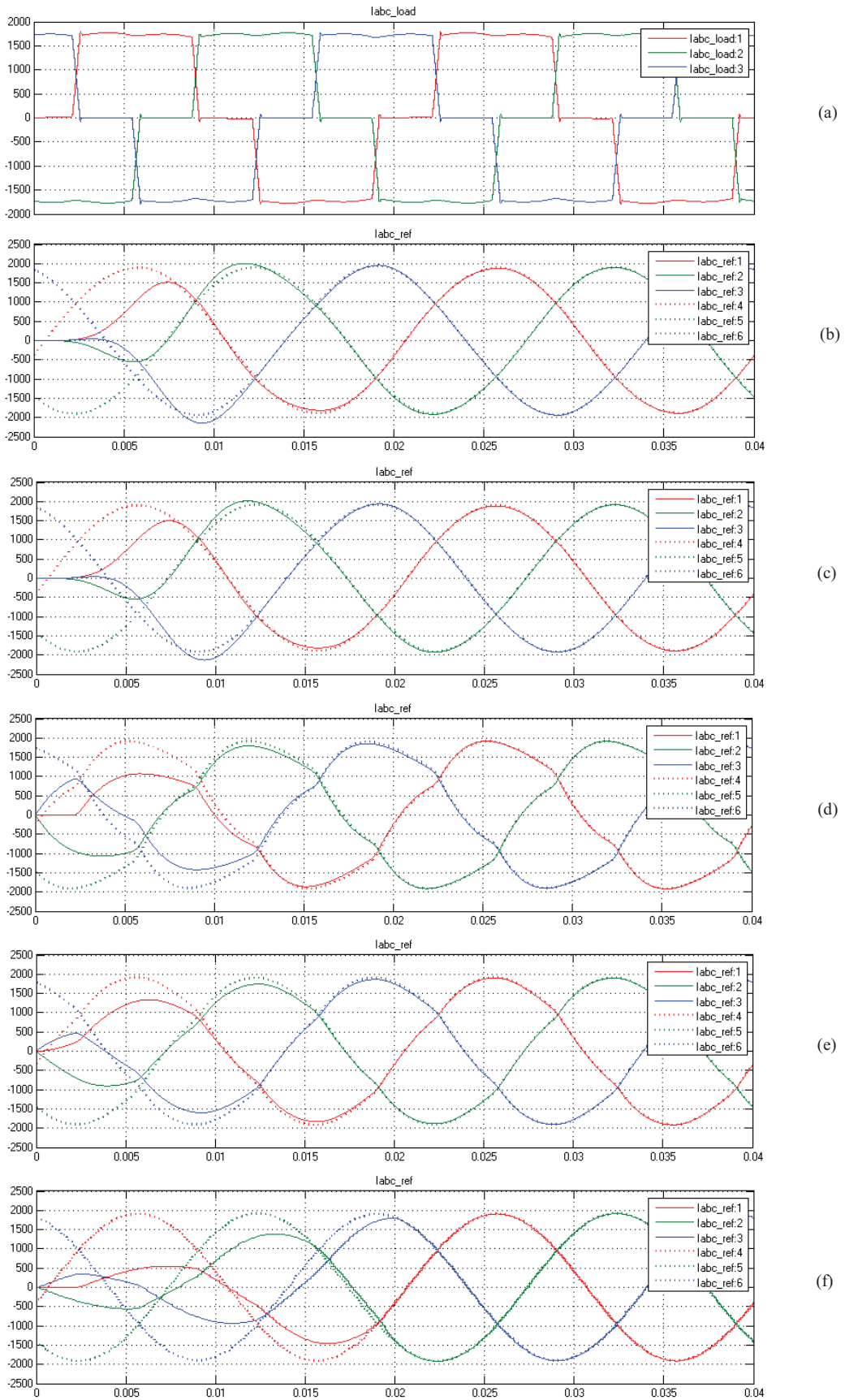


Fig. 11. Step response of the tested reference current detection methods: (a) load current; (b) IRP theory; (c) d-q reference frame; (d) SSI; (e) SSI+; (f) RDFT.

TABLE II.
COMPARISON OF APF REFERENCE CURRENT DETECTION METHODS UNDER DISTORTED AND UNBALANCED PCC VOLTAGES

Method	Settling time [ms]	THD I_{ref} [%]	THD I_{grid} [%]	THD V_{PCC} [%]	Overshoot [%]	Unbalance ^a [A]	Transient performance	DSP burden	Requirements for unbalanced and distorted V_{PCC}
IRP theory	12.5	1.28	3.21	7.25	12	42	high	low	SSI+ voltage filter
<i>d-q</i> SRF	12.5	0.95	3.22	7.23	11	24	high	low	SSI voltage filter for PLL
SSI ^b	16.5	5.95	5.5	7.4	0	15	medium	low	none, but the currents unbalance is inherited
SSI+ ^b	16.5	2.67	3.16	7.29	0	10	medium	double than simple SSI	none
RDFT	20	0.9	3.25	7.37	0	18	low	high	none, but the currents unbalance is inherited

^a Computed as difference between the lowest and the highest peak value of the three-phase currents, lower is better;

^b Tuned for an integral factor $k_i = 200$.

V. CONCLUSIONS

Some differences between the most common APF reference current detection methods under distorted and unbalanced PCC voltages were analyzed and tested in the Simulink environment, revealing their performance in non ideal real conditions (the static excitation system of a synchronous generator).

The author's choice for implementation is the *d-q* reference frame method because of the low THD reference current, good ability to deal with voltage unbalance, fast response time, high transient performance at thyristor firing angle change and relative low computational burden for the DSP. Also, the voltage phase vector can be used as well as an input to the P-SSI current controller with multiple SSI-s in synchronous reference frame.

ACKNOWLEDGMENT

This work was supported by the strategic grant POSDRU/159/1.5/S/133255, Project ID 133255 (2014), co-financed by the European Social Fund within the Sectorial Operational Program Human Resources Development 2007 – 2013.

REFERENCES

- [1] D. L. Popa, P. M. Nicolae, " Comparison of Active Power Filter Reference Current Detection Methods under Distorted and Unbalanced PCC Voltages", Proceedings of International Conference on Applied and Theoretical Electricity ICATE 2014, Craiova, Romania, oct. 2014.
- [2] E. H. Watanabe, M. Aredes, H. Akagi, "The p-q theory for active filter control: some problems and solutions", Sba Controle & Automação, vol. 15, no. 1, 2004, pp. 78–84.
- [3] Gary W. Chang, Tai-Chang Shee, "A Comparative Study of Active Power Filter Reference Compensation Approaches", IEEE 2002 Power Engineering Society Summer Meeting, vol. II, 2002, pp. 1017–1021.
- [4] P.-M. Nicolae, L.-D. Popa, M.-S. Nicolae, I.-D. Nicolae, "Instantaneous Power Theory applied to Power Conditioning under Distorted Mains Voltages: a MATLAB/Simulink Approach", 2014 International Power Electronics Conf. (IPEC-Hiroshima 2014 - ECCE-ASIA), 2014, pp. 2996–3001.
- [5] L. Asiminoaei, S. Hansen, C. Lascu, F. Blaabjerg, "Selective Harmonic Current Mitigation with Shunt Active Power Filter", 2007 European Conference on Power Electronics and Applications, 2007, pp. 1–10.
- [6] A. K. Guru, J. C. Balda, K. Carr, Y. Q. L. Xiang, "Design of a switching-ripple filter for a shunt-connected active power filter", The 1998 IEEE Industry Applications Conference, Thirty-Third IAS Annual Meeting, Vol. 2, 1998, pp. 1364–1368.
- [7] R. I. Bojoi, G. Griva, V. Bostan, M. Guerriero, F. Farina, F. Profumo, "Current control strategy for power conditioners using sinusoidal signal integrators in synchronous reference frame", IEEE Transactions on Power Electronics, Vol. 20, No. 6, 2005, pp. 1402–1412.
- [8] L. Limongi, R. Bojoi, G. Griva, A. Tenconi, "Comparing the Performance of Digital Signal Processor-Based Current Controllers for Three-Phase Active Power Filters", IEEE Industrial Electronics Magazine, Vol. 3, No. 1, 2009, pp. 20–31.
- [9] MATLAB and Simulink. Simulink R2014a. Developing S-Functions, MathWorks Inc. 2014, available online.
- [10] L. Asiminoaei, C. Lascu, I. Boldea, "Performance Improvement of Shunt Active Power Filter With Dual Parallel Topology", IEEE Transactions on Power Electronics, Vol. 22, No. 1, 2007, pp. 247–259.
- [11] L. Asiminoaei, F. Blaabjerg, S. Hansen, "Detection is key - Harmonic detection methods for active power filter applications", IEEE Industry Applications Magazine, vol. XIII, no. 4, 2007, p. 22–33.
- [12] H. Akagi, E. H. Watanabe, M. Aredes, Instantaneous power theory and applications to power conditioning, Wiley-Interscience, pp. 109–145, 2007.
- [13] X. Yuan, W. Merk, H. Stemmler, J. Allmeling, "Stationary-frame generalized integrators for current control of active power filters with zero steady-state error for current harmonics of concern under unbalanced and distorted operating conditions", IEEE Transactions on Industrial Applications, vol. XXXVIII, no. 2, 2002, pp. 523–532.
- [14] M. Machmoum, N. Bruyant, "DSP based control of shunt active power filters for global or selective harmonics compensation", Proc. of 9th International Conf. on Harmonics and Quality of Power, vol. II, 2000, pp. 661–666.
- [15] T. Komrska, J. Zak, Z. Peroutka, "Reactive power and harmonic currents compensation in traction systems using active power filter with DFT-based current reference generator", 13th European Conference on Power Electronics and Applications EPE '09, 2009, pp. 1–10.